

Mobilization of tin during continental subduction-accretion processes

Rolf L. Romer^{1*}, Uwe Kroner², C. Schmidt¹ and Claus Legler³

¹German Research Centre for Geosciences (GFZ), Telegrafenberg, D-14473 Potsdam, Germany

²Department of Geology, TU Bergakademie Freiberg, B.-v.-Cotta-Strasse 2, D-09596 Freiberg, Germany

³BEAK Consultants GmbH, Am St. Niclas Schacht 13, D-09599 Freiberg, Germany

ABSTRACT

Major tin (Sn) deposits within the Variscan orogen are closely related to 325–270 Ma postkinematic granites that intruded the metamorphic rocks of the former precollisional accretionary wedge of the Gondwana margin. In the Erzgebirge (Germany), some of these metasedimentary rocks have high Sn contents (locally more than 1000 ppm Sn). We report cassiterite (SnO₂) U-Pb ages of 395–365 Ma and high Sn contents in prograde biotite in these metasedimentary rocks. These data demonstrate that Sn was already introduced into these rocks during accretion and prograde metamorphism. Mobilization of Sn from sedimentary source rocks during prograde fluid loss in a subduction-accretion setting represents an important process of pre-enrichment of sedimentary source rocks that upon partial melting may produce Sn-enriched melts. The large-scale metamorphic mobilization of Sn, documented here for the first time, highlights the possible importance of metamorphic Sn enrichment in accretionary complexes, thereby explaining the spatial distribution of major Sn districts within the Variscan orogen.

INTRODUCTION

Tin (Sn) mineralization related to peraluminous granites is the result of a series of processes that operate in different tectonic settings. These processes include (1) residual enrichment of Sn during intense chemical weathering on a stable continent, (2) redistribution of the intensely weathered sediments to the continental margin during passive margin development, (3) stacking of the shelf sediments during the initial stages of accretion and collision in an active margin setting, (4) partial melting of subducted sedimentary rocks, (5) Sn enrichment in evolving granitic melts, (6) redistribution of Sn during fluid exsolution and during hydrothermal alteration of Sn-bearing granite, and (7) deposition of Sn in pegmatites and greisen, skarn, and lode types of mineralization (e.g., Lehmann, 1990; Romer and Kroner, 2015, 2022). This generic sequence of processes explains the distribution of granite-related tin deposits in belts along former continental margins and the broad range of mineralization ages within individual belts (Romer and Kroner, 2016, 2022). Tungsten (W) behaves similar to Sn during exogenic processes,

but it seems to take separate paths of redistribution during endogenic processes, as it may be mobilized during prograde metamorphism (e.g., Cave et al., 2017), partitions along with Li, Rb, and Cs into partial melts at lower temperature than Sn (e.g., Wolf et al., 2018; Yuan et al., 2019; Michaud et al., 2021), and seems to partition preferentially into the fluid during fluid exsolution, in contrast to Sn, which tends to stay in the melt (Schmidt et al., 2020). The contrasting behaviors of Sn and W explain why the two metals commonly are associated in the same mineral belt but typically occur in separate deposits (Yuan et al., 2019; Zhao et al., 2022).

The roles of most of the seven processes are increasingly well understood. For instance, chemical weathering results in the residual enrichment of Sn (and W) that is (are) adsorbed on or incorporated in clay minerals and Fe-oxyhydroxides and in the loss of Ca and Na, favoring the stabilization of mica rather than feldspar and amphibole during later metamorphism. The abundance of mica in turn allows for the formation and loss of a larger volume of low-Sn melt during early muscovite dehydration melting and a higher concentration of Sn in the restite (e.g., Wolf et al., 2018). The behavior of Sn during

early stages of subduction, however, is not well understood, even though it is a critical step in Sn redistribution.

We present chemical and U-Pb age data for cassiterite from a distinctive, highly sheared metasedimentary unit in the Erzgebirge, Germany, a major Variscan Sn province. We demonstrate that the high Sn content in the investigated sedimentary unit reflects fluid-related redistribution of Sn during the early stages of subduction-accretion of the metasedimentary rocks.

GEOLOGIC SETTING

The Variscan belt is the complex result of the collision between the continents of Gondwana and Laurussia, which included (1) tectonic reworking of the hyperextended West African part of the Gondwana shelf by ca. 400–340 Ma subduction-accretion processes, and (2) the final collision of these continents at ca. 340 Ma followed by the westward indentation of the East African–Arabian segment of the Gondwana shelf (Stephan et al., 2019a, 2019b; Kroner et al., 2022). Within the Variscan orogen, Sn deposits seem to occur in the former West African Gondwana shelf, and W deposits seem to occur mainly in the former East African–Arabian Gondwana shelf (Fig. 1A; Stephan et al., 2019b).

The Erzgebirge is a pile of nappes of metasedimentary rocks of the former passive margin West African Gondwana shelf (Fig. 1B). Early high-pressure metamorphism peaked at ca. 380 Ma, and high-pressure and ultrahigh-pressure metamorphism related to the continental collision peaked at 340 Ma (Klemd 2010; Hallas et al., 2021, and reference therein). The nappe pile was finally assembled during exhumation after 340 Ma and was intruded by crust-derived post-325 Ma granites (Förster and Romer, 2010). In the middle part of the nappe pile, there is a medium-pressure–low-temper-

*E-mail: romer@gfz-potsdam.de

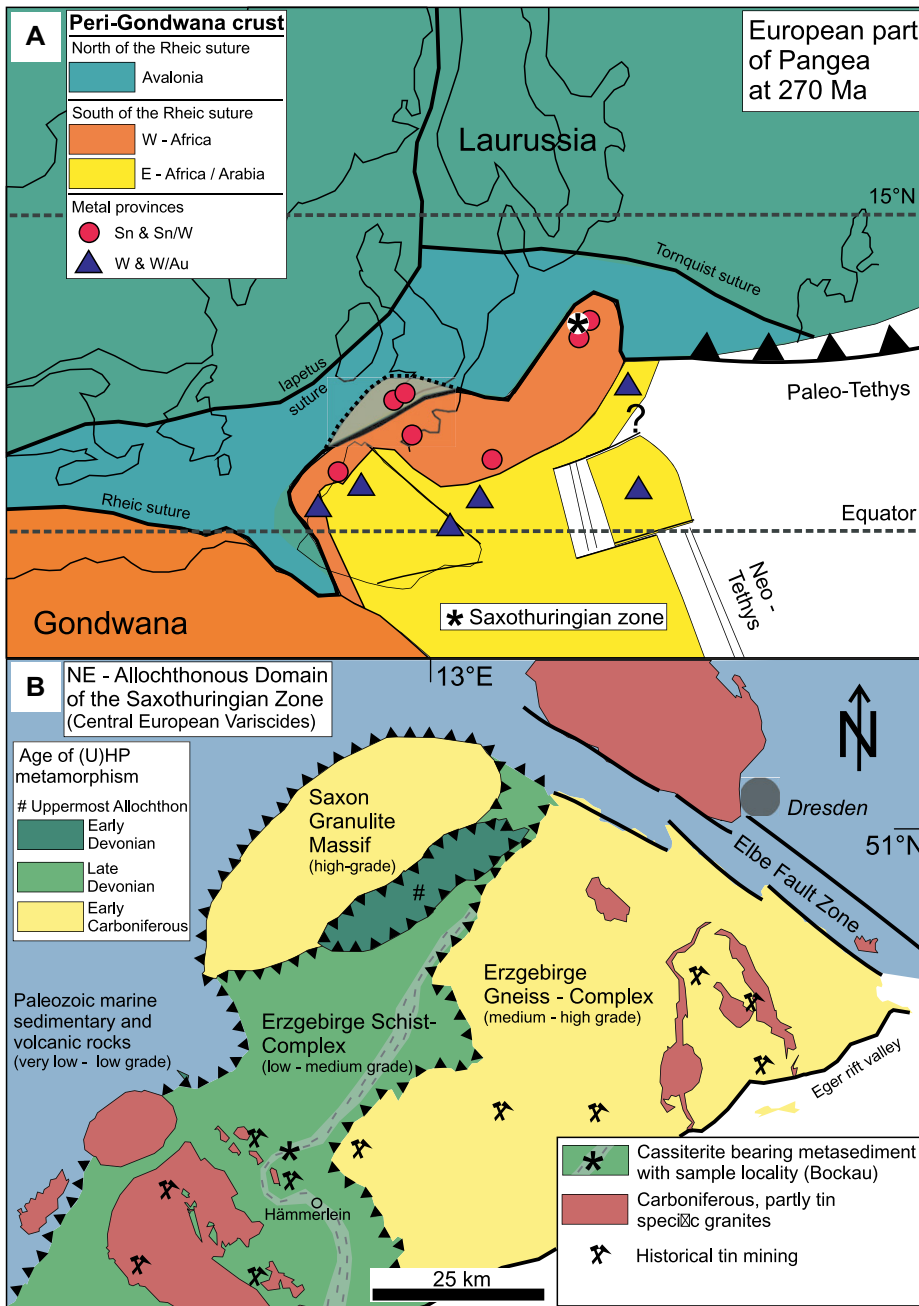


Figure 1. (A) Location of the Saxo-Thuringian zone within the Variscan orogen. Provenance of Paleozoic shelf sediments is according to Stephan et al. (2019a). Schematic distribution of Variscan Sn and W mineralization is taken from Stephan et al. (2019b). (B) Simplified tectonic map of Erzgebirge showing distribution of three differently aged nappe complexes, post-Variscan granites, historic mining activity, and anomalous Sn rocks of the Garnet Phyllite Unit, which dominantly consists of variably metamorphosed Ordovician sedimentary rocks (Mingram, 1998). (U)HP—(ultra)high pressure.

ature metasedimentary unit (Garnet Phyllite Unit) that mainly includes Early Ordovician quartzites, quartz phyllites, and phyllites of West African provenance (Mingram, 1998). The metamorphic mineral assemblage of these generally Al-Fe-rich rocks is typically feldspar-free (Rötzer et al., 1998; Jouvent et al., 2022). These metamorphic rocks are locally characterized by distinctly higher Sn contents (>1000 ppm) than their sedimentary protoliths (10–15 ppm; Romer and Hahne, 2010). In the Bockau and Aue areas

(Fig. 1B), metamorphic biotite and chlorite in these schists contain inclusions of metamorphic cassiterite. In addition, there are metamorphic quartz-cassiterite segregations (Fig. 2).

METAMORPHIC CASSITERITE FROM THE GARNET PHYLLITE UNIT, ERZGEBIRGE, GERMANY

We concentrated cassiterite (SnO₂) by dissolving ~400 g of two rock samples in HF on a hot plate. The purpose of using mineral acids

to concentrate cassiterite rather than crushing combined with traditional mineral separation procedures was to maximize cassiterite recovery, to get an idea of the grain-size distribution, and to preserve delicate overgrowth textures. Cassiterite was handpicked from the insoluble mineral residue (cassiterite plus some zircon) for electron microprobe analysis and U-Pb dating by isotope dilution–thermal ionization mass spectrometry. Analytical methods and results are provided in the Supplemental Material¹.

In the investigated samples, cassiterite occurs as inclusions in biotite and chlorite. Cassiterite forms small isolated grains with irregular shape (Figs. 2B and 2C). Some cassiterite has a radiating texture and appears to be porous and fractured (Fig. 2D). Electron microprobe data (see the Supplemental Material) showed low Fe and Ti contents typically below 1.1 wt% and 0.3 wt%, respectively, and slightly lower Fe and Ti contents at the rim (Figs. 2E and 2F; Table S1 in the Supplemental Material). The contents of Nb, Ta, and W were found to be near or below the detection limit. Cassiterite in biotite showed commonly lower Fe and Ti contents than cassiterite in chlorite. Biotite had high Fe and low Mg and Ti contents (Mg# = 29), as well as a relatively high Sn content (up to 0.08 wt% SnO₂). Chlorite was found to be Fe rich (Mg# = 24) and had a SnO₂ content below the detection limit (Tables S2 and S3). Thus, the retrograde formation of chlorite at the expense of biotite released Sn that may have precipitated as cassiterite, locally forming tiny inclusions in chlorite and radial overgrowths on silicate minerals and older cassiterite (Fig. 2).

Cassiterite inclusions in biotite gave a weighted apparent ²⁰⁶Pb/²³⁸U age of 395.3 ± 3.4 Ma (2σ), whereas cassiterite inclusions in chlorite gave a weighted ²⁰⁶Pb/²³⁸U apparent age of 367.8 ± 11.0 Ma (2σ) for the three fractions with the youngest apparent ²⁰⁶Pb/²³⁸U ages (Fig. 3; for discussion of analytical results, see the Supplemental Material). Cassiterite inclusions in chlorite (sample B1525R1) had lower ²⁰⁶Pb/²⁰⁴Pb ratios and higher U and Pb contents and yielded younger ²⁰⁶Pb/²³⁸U apparent ages. The older apparent ²⁰⁶Pb/²³⁸U ages of three fractions indicate that chloritization did not destroy cassiterite already present in the precursor biotite (Table S4). The older ages closely correspond to the age of onset of subduction and deformation in the accretionary wedge (Kroner and Romer, 2013). The younger age is clearly older than the age of granite magmatism (<325 Ma; Förster et al., 1999).

¹Supplemental Material. Analytical methods and U-Pb cassiterite data. Please visit <https://doi.org/10.1130/GEOL.S.20669298> to access the supplemental material, and contact editing@geosociety.org with any questions.

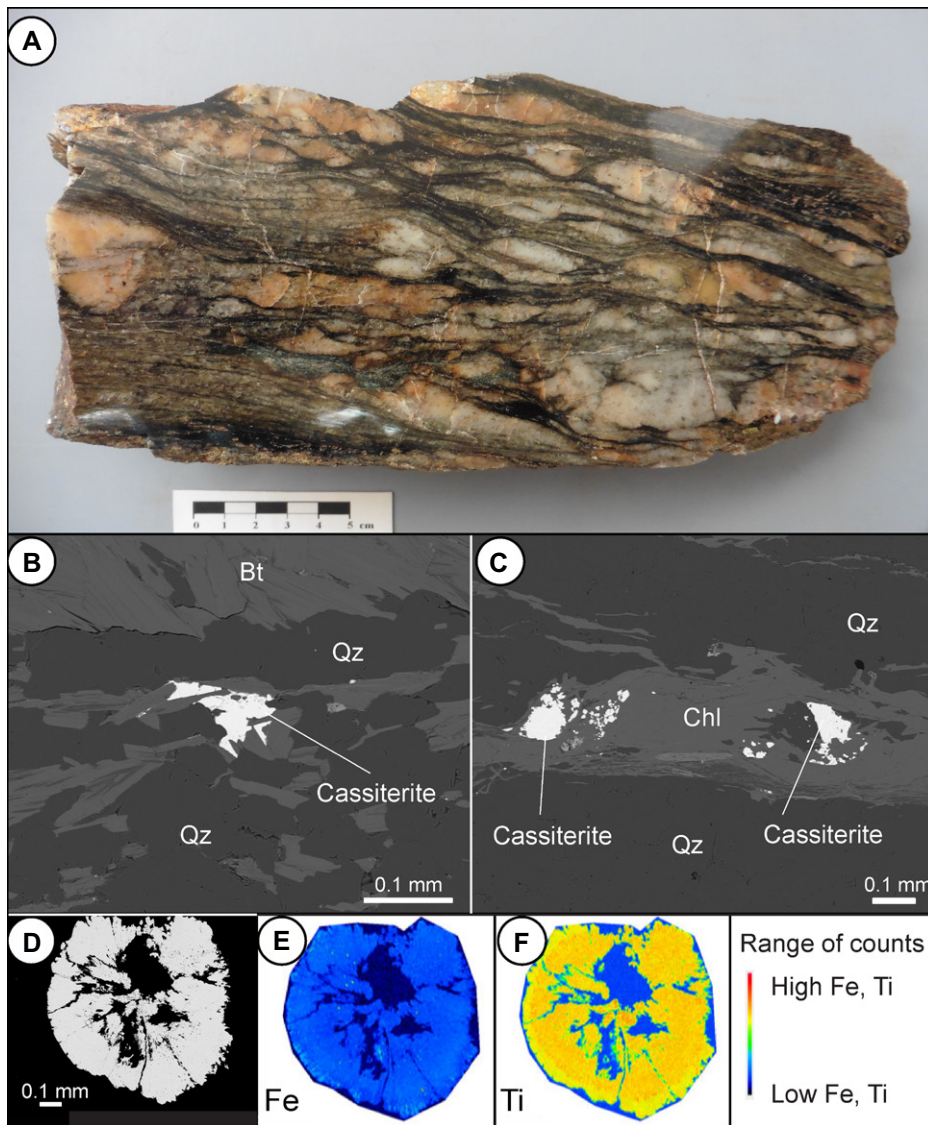


Figure 2. (A) Sheared quartz (Qz) segregations in mica schist with Sn-rich biotite. (B,C) Metamorphic cassiterite (SnO_2) in biotite (Bt; sample B1525R1) and chlorite (Chl; sample B1534R2), respectively. Note the irregular shape and small size of cassiterite in chlorite. (D) Backscattered electron (BSE) image of cassiterite crystal from sample B1534R2. Holes possibly represent former silicate inclusions that dissolved in HF during sample preparation. (E) Distribution of Fe. (F) Distribution of Ti.

DISCUSSION

The cassiterite inclusions in the metamorphic minerals demonstrate that the high Sn contents of the Garnet Phyllite Unit cannot be due to Sn additions from magmatic fluids from the postmetamorphic Sn-specific evolved granites. The cassiterite ages are not compatible with the presence of detrital cassiterite, the composition of which would not depend on the host rock. Instead, the age and composition of cassiterite and its occurrence as inclusions in Sn-rich biotite imply formation of cassiterite during prograde metamorphism. There are two types of metamorphic cassiterite, one in prograde biotite and one in retrograde chlorite. The older generation of cassiterite requires Sn addition by metamorphic fluids, whereas the younger gen-

eration reflects Sn release during chloritization of biotite.

The protoliths of the metamorphic rocks of the Garnet Phyllite Unit were chemically intensely weathered rocks that were characterized by low Ca and Na contents (e.g., Mingram, 1998), which resulted in feldspar-poor and feldspar-free metamorphic mineral assemblages (Rötzler et al., 1998). Sn released during chemical weathering on the continent became residually enriched by adsorption on clay minerals and Fe-oxyhydroxides. Later redeposition of these continental sediments on the marine Gondwanan shelf (Linnemann et al., 2000) accounted for high Cl contents in pore water of the sediments. During subduction and prograde metamorphism, clay minerals and Fe-oxyhydroxides from the

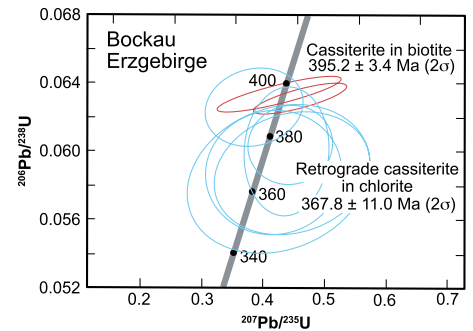


Figure 3. Concordia diagram for metamorphic cassiterite (SnO_2) from sample B1525R1 (red; biotite-hosted cassiterite) and B1534R2 (blue; chlorite-hosted cassiterite). Large 2σ uncertainties mainly reflect the unradiogenic nature of measured Pb and the uncertainty of common Pb isotopic compositions. For details, see the Supplemental Material (see footnote 1).

sedimentary protoliths were consumed to form micas and other silicate minerals. Adsorbed Sn ended up in the newly formed metamorphic minerals or in the pore fluids, where Sn formed chloride complexes. Subsequent metamorphic reactions redistributed Sn between the various metamorphic minerals and fluid. Whether this redistribution of Sn during prograde metamorphism reduced the Sn contents of the sedimentary rocks largely depended on the rock chemistry that determined the nature of stable metamorphic minerals, the partitioning of Sn between these minerals and fluids, the availability of Cl, and the temperature at fluid loss, as high temperatures increase Sn solubility (Schmidt, 2018). Compaction of the rock during subduction and prograde metamorphism resulted in the loss of pore water and metamorphic fluids (e.g., Fyfe et al., 1978; Yardley and Cleverley, 2015; Cave et al., 2017) together with dissolved Sn.

The chemical composition of the chemically intensely weathered sediments that are the dominant lithology of the metamorphic nappes of the Erzgebirge favored the formation of large amounts of Sn-poor, low-temperature melt by muscovite dehydration melting (Wolf et al., 2018), which resulted in Sn enrichment in the restite. Later melting of these restites generated Sn-specific granites (Wolf et al., 2018). The restricted mineral assemblage of these metasedimentary rocks, however, also may have favored the loss of Sn to a fluid when Sn-sequestering phases decomposed during prograde metamorphism. Loss of Sn during prograde metamorphism from geochemically favorable source rocks (e.g., Romer and Kroner, 2015, 2016) would have reduced the Sn endowment of these sedimentary rocks. On the other hand, the redistribution of Sn during prograde metamorphism may have increased the Sn contents of rocks that under normal circumstances would have little or

no potential to source Sn mineralization. Two examples of such rocks include (1) schists of the Garnet Phyllite Unit near Bockau, with Sn contents >1000 ppm Sn in some sections, and (2) metamorphic skarn-type mineralization at Hämmerlein (Fig. 1A).

Rocks of the Garnet Phyllite Unit near Bockau are characterized by high contents of Sn that is hosted in biotite (Table S2) and prograde and retrograde cassiterite (Fig. 2). The presence of prograde and retrograde cassiterite accounts for the broad range of cassiterite ages. The oldest ages for cassiterite (Fig. 3) indicate that Sn was mobile during prograde metamorphism. The younger ages (Fig. 3) demonstrate that Sn, as well as Fe and Ti, was released during chloritization and incorporated in the second generation of cassiterite. The redistribution of Sn during subduction-accretion and metamorphism may have resulted in very high Sn contents in units that served as fluid channels. Although this process is so far not known to form economic Sn mineralization, it definitively has the potential to produce highly fertile protoliths that upon partial melting may produce Sn-rich melts, even without significant magmatic fractionation. Metamorphic redistribution of Sn during subduction-accretion processes affected the western segment of the Gondwana shelf, where the major Variscan Sn provinces of Cornwall, Erzgebirge, and Galicia developed, but were absent in the eastern segment of the Gondwana shelf, where W rather than Sn deposits formed (Stephan et al., 2019b).

Within the Erzgebirge, there are numerous skarn deposits, some of which host significant resources of Sn, Zn, and In (e.g., Bauer et al., 2019; Lefebvre et al., 2019a). There were two events of Sn addition: first, Sn redistributed during Variscan metamorphism was sequestered in metamorphic minerals of the peak assemblage (garnet, pyroxene, and amphibole) that may have had Sn contents as high as 1 wt% (Lefebvre et al., 2019a). Second, the emplacement of postmetamorphic Variscan granites may have introduced additional Sn and induced chloritization of minerals of the peak metamorphic assemblage, thereby releasing Sn that precipitated as cassiterite (Lefebvre et al., 2019a). A comparison of the skarns and their nonmineralized equivalents indicated that addition of Sn was associated with the addition of Fe, Zn, As, (W), Sc, and In (Lefebvre et al., 2019b). Thus, the high Sn content in minerals of the metamorphic peak assemblage demonstrates that Sn (as well as Fe, Zn, As, and In) was transported by metamorphic fluids. The enrichment of these elements in skarn rocks indicates that their precipitation may have been strongly affected by fluid-driven reactions between silicate and carbonate rocks that (1) resulted in the formation of the skarn mineral assemblages and (2) modified the fluid composition, which resulted

in the incorporation of Sn in silicate minerals (Lefebvre et al., 2019b).

SUMMARY

High Sn contents in metamorphic minerals and cassiterite U-Pb ages of 395–365 Ma demonstrate that the high Sn concentrations in some metamorphic rocks of the Erzgebirge are not related to the emplacement of the 325–300 Ma postkinematic Sn granites. Instead, Sn was redistributed during prograde fluid loss in a subduction-accretion setting. Metamorphic mobilized Sn may have precipitated in shear zones (locally >1000 ppm Sn) and along reaction fronts with carbonate rocks (as in the Hämmerlein skarn). Retrogression of Sn-rich silicates would have released Sn and formed secondary cassiterite. Metamorphic mobilization of Sn from sedimentary source rocks during prograde fluid loss in a subduction-accretion setting may represent an important Sn enrichment step of sedimentary source rocks that upon partial melting may produce Sn-enriched melts. Metamorphic redistribution of Sn during subduction may be important beyond the Erzgebirge: Variscan Sn deposits occur in rocks of the former West African shelf and are generally absent in rocks of the former East African–Arabian shelf (Stephan et al., 2019b). The West African shelf experienced extensive subduction-accretion before the final collision of Laurussia and Gondwana, whereas the East African–Arabian shelf did not.

ACKNOWLEDGMENTS

We thank Oona Appelt (GFZ) for the electron microprobe analyses. We thank Robin Shail, Mike Searle, and two anonymous reviewers and the editor, Gerald Dickens, for helpful comments.

REFERENCES CITED

- Bauer, M.E., Seifert, T., Burisch, M., Krause, J., Richter, N., and Gutzmer, J., 2019, Indium-bearing sulfides from the Hämmerlein skarn deposit, Erzgebirge, Germany: Evidence for late-stage diffusion of indium into sphalerite: *Mineralium Deposita*, v. 54, p. 175–192, <https://doi.org/10.1007/s00126-017-0773-1>.
- Cave, B.J., Pitcairn, I.K., Craw, D., Large, R.R., Thompson, J.M., and Johnson, S.C., 2017, A metamorphic mineral source for tungsten in the turbidite-hosted orogenic gold deposits of the Otago Schist, New Zealand: *Mineralium Deposita*, v. 52, p. 515–537, <https://doi.org/10.1007/s00126-016-0677-5>.
- Förster, H.-J., and Romer, R.L., 2010, Carboniferous magmatism, in Linnemann, U., and Romer, R.L., eds., *Pre-Mesozoic Geology of Saxo-Thuringia—From the Cadomian Active Margin to the Variscan Orogen*: Stuttgart, Germany, Schweizerbart, p. 287–308.
- Förster, H.J., Tischendorf, G., Trumbull, R.B., and Gottesmann, B., 1999, Late-collisional granites in the Variscan Erzgebirge, Germany: *Journal of Petrology*, v. 40, p. 1613–1645, <https://doi.org/10.1093/ptro/40.11.1613>.
- Fyfe, W.S., Price, N.J., and Thompson, A.B., 1978, Fluids in the Earth's Crust: Amsterdam, Elsevier, 383 p.

- Hallas, P., Pfänder, J.A., Kroner, U., and Sperner, B., 2021, Microtectonic control of ⁴⁰Ar/³⁹Ar white mica age distributions in metamorphic rocks (Erzgebirge, N-Bohemian Massif): Constraints from combined step heating and multiple single grain total fusion experiments: *Geochimica et Cosmochimica Acta*, v. 314, p. 178–208, <https://doi.org/10.1016/j.gca.2021.08.043>.
- Jouvent, M., Lexa, O., Peřestý, V., and Jeřábek, P., 2022, New constraints on the tectonometamorphic evolution of the Erzgebirge orogenic wedge (Saxothuringian domain, Bohemian Massif): *Journal of Metamorphic Geology*, v. 40, p. 687–715, <https://doi.org/10.1111/jmg.12643>.
- Klemd, R., 2010, The early Variscan allochthonous domains: The Münchberg Complex, Frankenberg, Wildenfels, and Góry Sowie, in Linnemann, U., and Romer, R.L., eds., *Pre-Mesozoic Geology of Saxo-Thuringia—From the Cadomian Active Margin to the Variscan Orogen*: Stuttgart, Germany, Schweizerbart, p. 221–232.
- Kroner, U., and Romer, R.L., 2013, Two plates—Many subduction zones: The Variscan orogeny reconsidered: *Gondwana Research*, v. 24, p. 298–329, <https://doi.org/10.1016/j.gr.2013.03.001>.
- Kroner, U., Stephan, T., and Romer, R.L., 2022, Paleozoic orogenies and relative plate motions at the sutures of the Iapetus-Rheic Ocean, in Kuiper, Y.D., et al., eds., *New Developments in the Appalachian-Caledonian-Variscan Orogen*: Geological Society of America Special Paper 554, p. 1–23, [https://doi.org/10.1130/2021.2554\(01\)](https://doi.org/10.1130/2021.2554(01)).
- Lefebvre, M.G., Romer, R.L., Glodny, J., Kroner, U., and Roscher, M., 2019a, The Hämmerlein skarn-hosted polymetallic deposit and the Eibenstock granite associated greisen, western Erzgebirge, Germany: Two phases of mineralization—Two Sn sources: *Mineralium Deposita*, v. 54, p. 193–216, <https://doi.org/10.1007/s00126-018-0830-4>.
- Lefebvre, M.G., Romer, R.L., Glodny, J., and Roscher, M., 2019b, Skarn formation and tin enrichment during regional metamorphism: The Hämmerlein polymetallic skarn deposit: *Lithos*, v. 348–349, <https://doi.org/10.1016/j.lithos.2019.105171>.
- Lehmann, B., 1990, *Metallogeny of Tin*: Berlin, Springer-Verlag, 212 p.
- Linnemann, U., Gehmlich, M., Tichomirowa, M., Buschmann, B., Nasdala, L., Jonas, P., Lützner, H., and Bombach, K., 2000, From Cadomian subduction to early Palaeozoic rifting: The evolution of Saxo-Thuringia at the margin of Gondwana in the light of single zircon geochronology and basin development (Central European Variscides, Germany), in Franke, W., et al., eds., *Orogenic Processes: Quantification and Modelling in the Variscan Belt*: Geological Society, London, Special Publication 179, p. 131–153, <https://doi.org/10.1144/GSL.SP.2000.179.01.10>.
- Michaud, J.A.S., Pichavant, M., and Villaros, A., 2021, Rare elements enrichment in crustal peraluminous magmas: Insights from partial melting experiments: *Contributions to Mineralogy and Petrology*, v. 176, 96, <https://doi.org/10.1007/s00410-021-01855-9>.
- Mingram, B., 1998, The Erzgebirge, Germany, a subducted part of northern Gondwana: Geochemical evidence for repetition of early Palaeozoic metasedimentary sequences in metamorphic thrust units: *Geological Magazine*, v. 135, p. 785–801, <https://doi.org/10.1017/S0016756898001769>.
- Romer, R.L., and Hahne, K., 2010, Life of the Rheic Ocean: Scrolling through the shale record: *Gondwana Research*, v. 17, p. 236–253, <https://doi.org/10.1016/j.gr.2009.09.004>.
- Romer, R.L., and Kroner, U., 2015, Sediment and weathering control on the distribution of

- Paleozoic magmatic tin-tungsten mineralization: Mineralium Deposita, v. 50, p. 327–338, <https://doi.org/10.1007/s00126-014-0540-5>.
- Romer, R.L., and Kroner, U., 2016, Phanerozoic tin and tungsten mineralization—Tectonic controls on the distribution of enriched protoliths and heat sources for crustal melting: Gondwana Research, v. 31, p. 60–95, <https://doi.org/10.1016/j.gr.2015.11.002>.
- Romer, R.L., and Kroner, U., 2022, Provenance control on the distribution of endogenic Sn-W, Au, and U mineralization within the Gondwana-Laurussia plate boundary zone, in Kuiper, Y.D., et al., eds., New Developments in the Appalachian-Caledonian-Variscan Orogen: Geological Society of America Special Paper 554, p. 25–46, [https://doi.org/10.1130/2021.2554\(02\)](https://doi.org/10.1130/2021.2554(02)).
- Rötzler, K., Schumacher, R., Maresch, W.V., and Willner, A.P., 1998, Characterization and geodynamic implications of contrasting metamorphic evolution in juxtaposed high-pressure units of the western Erzgebirge (Saxony, Germany): European Journal of Mineralogy, v. 10, p. 261–280, <https://doi.org/10.1127/ejm/10/2/0261>.
- Schmidt, C., 2018, Formation of hydrothermal tin deposits: Raman spectroscopic evidence for an important role of aqueous Sn(IV) species: Geochimica et Cosmochimica Acta, v. 220, p. 499–511, <https://doi.org/10.1016/j.gca.2017.10.011>.
- Schmidt, C., Romer, R.L., Wohlgemuth-Ueberwasser, C., and Appelt, O., 2020, Partitioning of Sn and W between granitic melt and aqueous fluid: Ore Geology Reviews, v. 117, <https://doi.org/10.1016/j.oregeorev.2019.103263>.
- Stephan, T., Kroner, U., and Romer, R.L., 2019a, The pre-orogenic detrital zircon record of the Peri-Gondwana crust: Geological Magazine, v. 156, p. 281–307, <https://doi.org/10.1017/S0016756818000031>.
- Stephan, T., Kroner, U., Romer, R.L., and Rösel, D., 2019b, From a bipartite Gondwana shelf to an arcuate Variscan belt: The early Paleozoic evolution of northern Peri-Gondwana: Earth-Science Reviews, v. 192, p. 491–512, <https://doi.org/10.1016/j.earscirev.2019.03.012>.
- Wolf, M., Romer, R.L., Franz, L., and López-Morro, F.J., 2018, Tin in granitic melts: The role of melting temperature and protolith composition: Lithos, v. 310–311, p. 20–30, <https://doi.org/10.1016/j.lithos.2018.04.004>.
- Yardley, B.W., and Cleverley, J.S., 2015, The role of metamorphic fluids in the formation of ore deposits, in Jenkin, G.R.T., et al., eds., Ore Deposits in an Evolving Earth: Geological Society, London, Special Publication 393, p. 117–134, <https://doi.org/10.1144/SP393.5>.
- Yuan, S.D., Williams-Jones, A.E., Romer, R.L., Zhao, P.L., and Mao, J.W., 2019, Protolith-related thermal controls on the decoupling of Sn and W in Sn-W metallogenic provinces: Insights from the Nanling region, China: Economic Geology, v. 114, p. 1005–1012, <https://doi.org/10.5382/econgeo.4669>.
- Zhao, P., Yuan, S., Williams-Jones, A.E., Romer, R.L., Yan, C., Song, S., and Mao, J., 2022, Temporal separation of W and Sn mineralization by temperature-controlled incongruent melting of a single protolith: Evidence from the Wangxianling area, Nanling region, South China: Economic Geology, v. 117, p. 667–682, <https://doi.org/10.5382/econgeo.4902>.

Printed in USA